ISBN: 978-628-95207-4-3. ISSN: 2414-6390. Digital Object Identifier: https://dx.doi.org/10.18687/LACCEI2023.1.1.664

Non-destructive evaluation of dry matter in 'Edward' mango by reflectance spectroscopy

Ernesto Paiva-Peredo, MSc.[1], Renzo Morales-Hualla, Student[1], Isrrael Gálvez-Porras, Student[1], and Wiliam Trujillo, PhD[1].
[1]Universidad Tecnológica del Perú, Peru, epaiva@utp.edu.pe, U17104628@utp.edu.pe, 1221502@utp.edu.pe, wtrujillo@utp.edu.pe

Abstract*– Mango is a very popular climacteric fruit in America and Europe. Within the internal properties of mango, dry matter is a suitable indicator to estimate the final quality of mango, however, the measurement of this indicator requires destructive testing and high time consumption. Therefore, this research creates a new spectral database of Edward mango to build models based on Partial Least Squared Regression (PLSR) and Principal Component Regression (PCR). Our research analyzes a total of 18 PCR models and 18 PLSR models, where 4 types of transformations on the dependent variable (logarithmic, square root, square and none transformation), 3 types of reflectance-based feature extractors (logarithmic, first derivative and none transformation), and 3 preprocessing techniques (Standard Normal Variate (SNV), Multiplicative Signal Correction (MSC) and none preprocessing) have been studied. The research proposes a double cross-validation both to determine the optimal number of components and to obtain the final metrics. The best model has an RMSE of 1.6142 %MS and an RMSE of 0.6102 in the scaled dimension. The model used 3 components, did not use transformation, used R reflectance as the independent variable and MSC as the preprocessing technique.

Keywords—Spectroscopy, Machine learning, Partial least squares, Principal component analysis, Dry matter

I. Introduction

Since 2002, fresh mango has been one of the most exported fruit in Peru and is the fourth most exported Peruvian fruit. The Peruvian Ministry of Foreign Trade and Tourism indicates that there are 4 main difficulties in mango production and export. Two of them are poor technological development and limited technical assistance to improve mango production and quality. Traditional techniques used to determine fruit maturity are destructive and cause delays in production.

Mango is a climacteric fruit that is generally harvested at the hard green stage, which facilitates the time to move and sell it [1], [2]. Mango fruit is traded in the market by quality categories. In the past, skin color, fruit size and shape were the most common quality determinants [3]–[5], but now characteristics related to internal and nutritional quality are very influential in the consumer's decision [6]. Dry matter (DM) is a fundamental quality characteristic in fresh fruit that facilitates judging its maturity [7]–[9].

To determine the internal quality of mango, a destructive procedure executed by trained personnel is required, which generates high analysis costs and does not allow inspecting the entire production [10]–[12]. Currently, new technologies based on nondestructive methods are used to help predict mango quality and maturity, such as nuclear magnetic resonance (NMR) [13], impact response [14], electronic nose [15], hyperspectral analysis [16]–[18] and near infrared (NIR) spectroscopy [6], [7], [10], [19]–[21]. Spectroscopy has been used in various applications such as the detection of explosives [22], adulteration of food products [23] and the detection of substances [24].

In NIR spectroscopy of fresh fruit, the interaction with light produces two main phenomena, absorbance, and reflectance. The absorbance is associated with the chemical components that are present in the fresh fruit, while the reflectance is caused by the physical microstructure of the skin and pulp of the fruit.

Lately, there is a growing interest in the use of advanced machine learning algorithms, such as deep learning, to model spectral data. Interest in deep learning (DL) is growing because it continues to learn as data increases, whereas traditional machine learning algorithms are locked at a certain point [25].

Fruit ripening is a process involving changes in physical and biochemical properties. DM is a chemical parameter and is used to determine the edible quality of the fruit. This variable is measured in percentage and remains constant at a certain ripening stage, and then increases indicating water loss. Its value depends not only on the species, but also on the crop and climate where it is grown or stored. In [26] the DM in mango was analyzed, obtaining values from 9.5 to 15.8%. A stable value (15.8%) indicates optimal mango quality for sale. However, not all the parameters have the same efficiency or capacity to determine both maturity and quality in the ripening process of a fruit.

In [27], the effectiveness of DM, total soluble solid (TSS), titratable acidity (TA), and peel color (PC) at harvest and postharvest of Cogshall mango in determining maturity and shelf life was compared. The study concludes that DM indicates if the mango will be of quality when it reaches its maximum maturity. In summary, MD is a parameter that indicates mango quality at harvest and postharvest in a controlled environment [6], [26]–[28].

It is of interest to predict maturity without resorting to destructive techniques. For this purpose, NIR spectroscopy is used. There are several applications, each with different wavelength ranges. The visible and near infrared spectroscope (VIS-NIR) model F-750 with a wavelength range of 306 to 1140 nm was applied to the Palmer mango. This has the characteristic of having red and green external spots.

Digital Object Identifier: (only for full papers, inserted by LACCEI).
ISSN, ISBN: (to be inserted by LACCEI).
DO NOT REMOVE

Observations in [11] indicate that red pigments are found between 625-740 nm and green pigments between 500-565 nm. These green regions are the ones that affect mango spectra and are recurrent in immature mangoes. Then, if it is desired to identify DM, a range between 625-740 nm should be occupied, since red mangoes are those that are ripe [11]. Research [28] analyzes it with a time reflectance spectroscopic technique (TRS) to three types of mangoes: Haden, Palmer and Tommy Atkins. The results were like the previous investigation [28], since the green layer attenuates the spectrometer signal. Then another length must be resorted to, in this case from 650 nm to 690 nm. If the red layer predominates in the case, a length of 540 nm to 900 nm is used. Immature mangoes have a high chlorophyll content. In contrast, mature mangoes have these reddish spots due to the appearance of carotenoids [28]. In a recent investigation [29], a VIS-NIR spectrometer model USB4000 with a range of 300-1000 nm is used. The objective is to determine maturity from dry matter and soluble solids. There is an absorbance in green mangoes and in this case, interference is perceived at 675 nm. To identify DM, it is analyzed at values close to 914-916 nm. Then, NIR spectroscopy can estimate mango maturity accurately, only if the type of mango and the maturity stage are taken as a condition; at harvest and postharvest [11], [28], [29].

Once the data have been obtained, it must be analyzed to indicate and estimate the degree of ripeness. Partial least squares regression (PLS) or principal component analysis (PCA) is used for this purpose. However, some authors make prior use of multiple linear regression (MLR). In their case, they establish NIR calibration equations to determine starch and dry matter. From that, they predict soluble solids and, therefore, fruit sweetness upon consumption [30]. Finally, the PLS model is most effective when the mango is of the same cultivar. For example [31], when it is decided to compare MLR and PLS to determine which one better predicts a maturity index, developed based on physicochemical properties. First, MLR obtains higher correlation coefficient (R) values than PLS regression. However, when the calibration and validation standard deviation is calculated, it is shown that PLS has higher accuracy. It is concluded, that the PLS model is used in research that aims to predict the maturity of a fruit, but if higher accuracy of the results is desired, pre-processing with other regression models should be performed [30]–[32].

In summary, dry matter is effective physicochemical parameters for indicating and predicting mango ripeness. If quality is sought, dry matter is more relevant, since this parameter is also used to infer TSS, an indicator of fruit sugar. In addition, NIR spectroscopy can indicate mango maturity and quality, although it depends on the choice of a range of lengths. Finally, PLS regression model predicts mango maturity and quality, based on spectral samples taken at harvest and destructive tests performed throughout the shelf life. In this way, it seeks to relate both data and establish a prediction. However, if you want to be more accurate, preprocessing is required. Finally, research have been found mainly with Kent mangoes. However, no research has been reported where Edwards mango models have been built with NIR spectroscopy.

Therefore, in this research, different pre-processing and transformation techniques are studied using spectral signatures in the NIR range to create PLSR and PCA models with the aim of predicting the dry matter of an Edward mango with a faster and non-destructive approach.

II. Method

Fig. 1 shows the methodology implemented. The methodology has been divided into 4 phases. Spectral data collection and DM measurement, a pre-processing stage of the raw data, a double cross validation (CV) stage and finally a testing phase to obtain the model metrics.

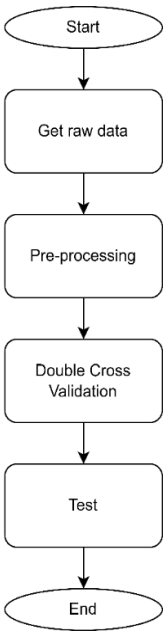

Fig. 1 Methodology flowchart

A. Collection of spectral signatures

Spectral signature recording was performed with an AvaSpec-NIR256-1.7-EVO NIR spectrometer in reflectance mode. The spectrometer has an operating spectral range of 900 to 1750 nm with 221 bands.

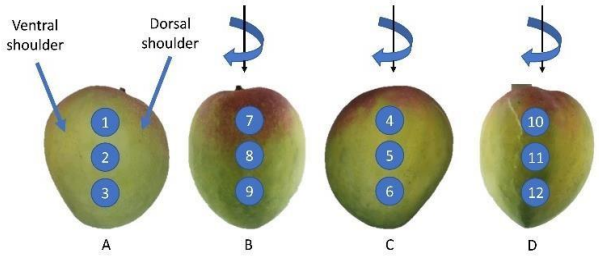

Fig. 2 Location of measurement points. A) Morphology of the mango and location of points 1, 2 and 3. B) Location of points 7, 8 and 9. C) Location of points 4, 5 and 6. D) Location of points 10, 11 and 12

Eighteen Edward variety mangoes have been sampled; however, 12 measurement points have been identified on each of them, making a total of 216 samples. The location of the measurement points is determined by a measurement protocol detailed in Fig. 2. First, the mango is placed with the dorsal shoulder to the right, then 3 circles are marked at different levels on the cheek of the mango as shown in Fig. 2A. Subsequently, the mango is turned 90 degrees and 3 new areas are marked at different levels as shown in Fig. 2. The procedure is repeated as shown in Figure 2C and Figure 2D.

B. DM measurement

A measurement of the amount of dry matter per mango was carried out due to the high time consumption of the drying procedure. The experiment used a Radwag MA 50.R moisture analyzer with a readability of 1 mg.

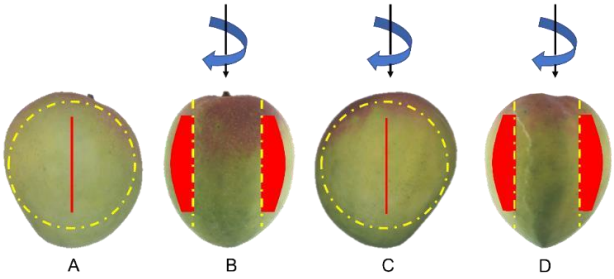

Fig. 3 Detail of dry matter sample strands extracted from the mango.

DM was estimated from two slices of pulp from both mango cheeks. First, two longitudinal cuts were made without touching the mango pulp. Subsequently, a slice was taken from each cheek as shown in Fig. 3. Yellow dotted lines represent the cut cheeks in A, B, C and D. The red solid lines show the extracted slices in their lateral view in A and C. The red filled areas show the slices extracted in their front view in B and D.

C. Pre-processing

A flow chart of the pre-processing stage is detailed in Fig. 4. First, the dependent variable went through a transformation substage (logarithmic, square root, power of two or no transformation).

On the other hand, the independent variables (see Fig. 5A) went through a filtering sub-stage applying a Savitzky-Golay filter with a 7-point window and a second-degree polynomial (see Fig. 5B)

The filtered independent variable went through a transformation substage (logarithmic, first derivative or no transformation). The first derivative was calculated by applying a Savitzky-Golay filter with a 7-point window and a second-degree polynomial.

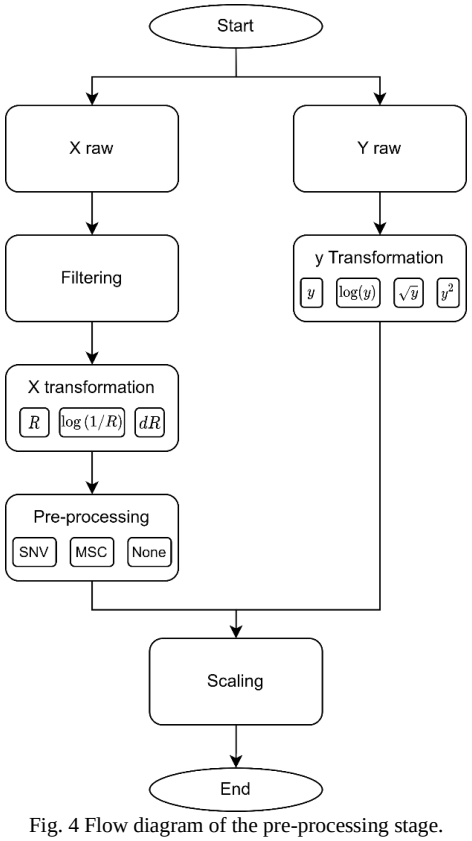

Fig. 4 Flow diagram of the pre-processing stage.

The most used smoothing and differencing technique in chemometrics is the Savitzky-Golay method [33]–[35], which consists of a local polynomial regression requiring equidistant spectrum values, as shown in (1).

$$x_j^* = \frac{1}{N}\sum_{h=-k}^{k} c_h x_{j+h} \quad (1)$$

Where, x_j^* is the value of the curve to be smoothed or derived. N is the number of points in the window. k is the number of neighboring points per side. c_h are the coefficients that depend on the degree of the regression polynomial and the objective (smoothed or derived).

Additionally, transformed independent variables were passed to a pre-processing substage. In this stage, one of the following techniques was applied: Standard Normal Variate (SNV), Multiplicative Signal Correction (MSC) or none of the above. As example, you can see Fig. 5C, where SNV is applied to Fig. 5B.

Finally, the independent and dependent variables went to a scaling stage of mean removal and unit variance standardization. As example, you can see Fig. 5D, where scaling is applied to Fig. 5C.

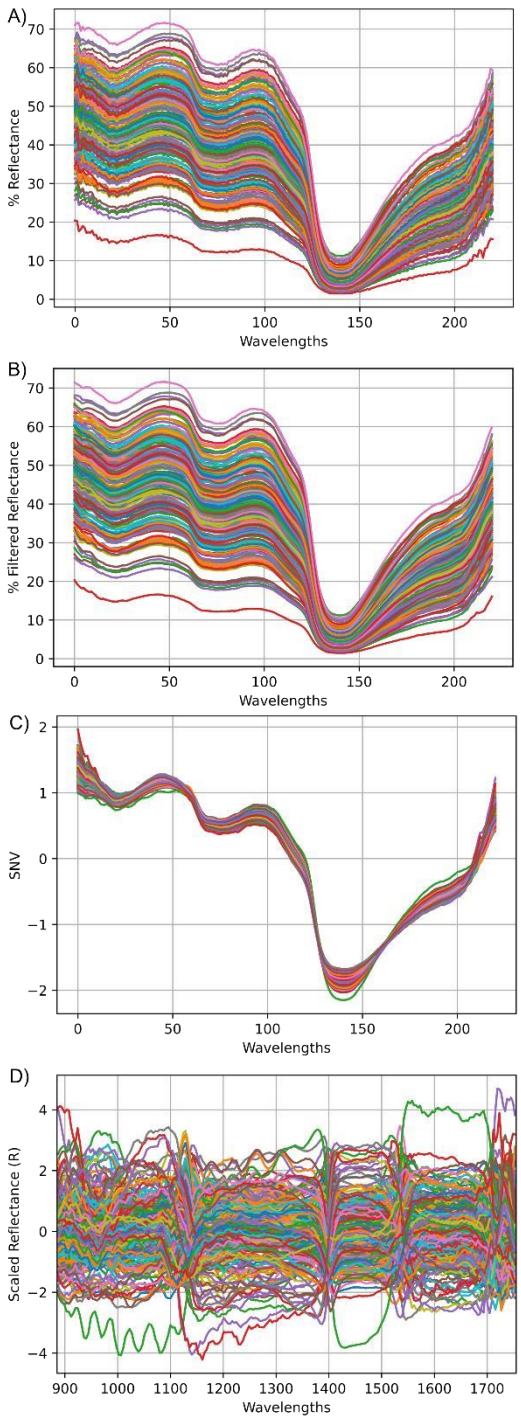

Fig. 5 A) Raw reflectance measurements. B) Filtered reflectance applying a Savitzky-Golay filter. C) SNV result as pre-processing technique- D) Output of scaling phase.

D. Double CV with repetitions

A schematic of the double CV is explained in Fig. 6. The internal CV defines the training and validation sets; and the optimal number of a_{opt} components. The inner CV is repeated 50 times, resulting in a list of 50 a_{opt}. The external CV defines the test and calibration sets. Each external segmentation obtains the list of 50 a_{opt}. At the end the s_{OUT} lists are grouped.

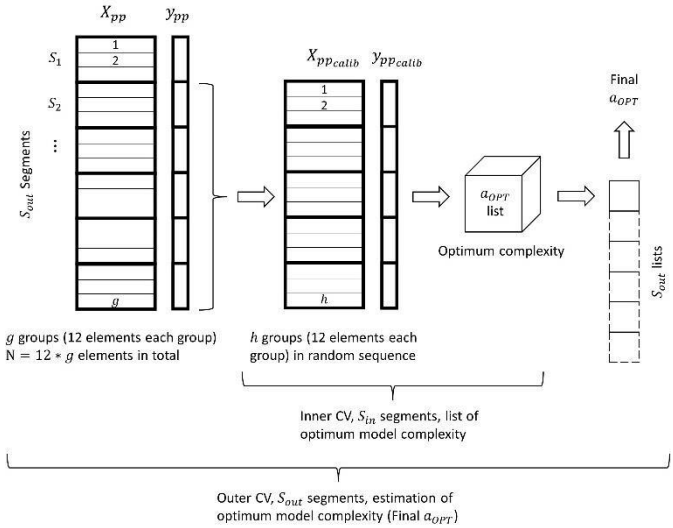

Fig. 6 Double CV with $s_{OUT} = 4$ segments in the outer CV and $s_{IN} = 10$ segments in the inner CV executed to obtain the a_{opt}.

A crucial point to build a predictive model with PCR or PLSR is to decide the number of components to be used. In principle, previously the independent variables can pass a variable selection stage, however for simplicity the project is limited to finding the optimal number of components a_{opt}.

In the internal CV, the calibration set was divided into training and validation sets. The 12 samples from each handle were combined, shuffled and finally distributed in the same set to avoid false optimistic results.

The selection of the optimal number of principal components is based on one standard error rule. Finally, the s_{OUT} lists of 50 candidates of optimal number of components were analyzed using a histogram. The final a_{opt} is determined by calculating the mode of the candidates.

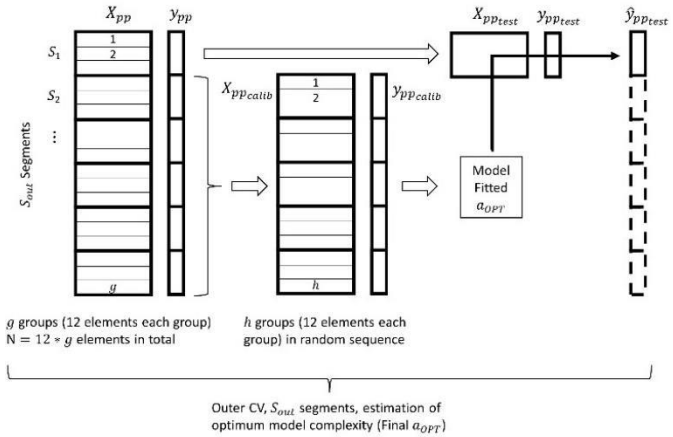

Fig. 7 Double CV with s_{OUT} segments in the external CV executed to obtain test predictions of all data.

E. Double CV with repetitions

The external CV is rerun to build a model with a_{opt} components. The training uses the entire calibration set and makes predictions from the test set. The procedure is repeated for the other CV segmentations until the prediction of all data is completed as shown in Fig. 7.

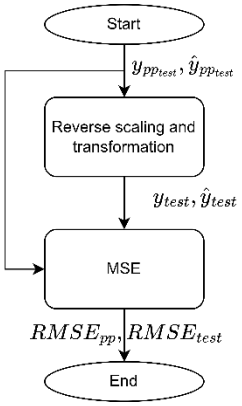

Fig. 8 RMSE calculation flowchart.

The result of the procedure explained in Fig. 8 are the test set predictions scaled by the pre-processing stage and $\hat{y}_{pp_{test}}$, that attempt to fit $y_{pp_{test}}$. In addition, $y_{pp_{test}}$ and $\hat{y}_{pp_{test}}$ went through an inversion of the previous scaling and transformation to obtain y_{test} and $\hat{y}_{test}$. Finally, applying the following equation yields $RMSE_{pp}$ and $RMSE_{test}$.

III. Results and Discussion

The method presented consisted of evaluating 4 transformations, 3 types of features and 3 pre-processing techniques, that is, 36 models as shown in Table I.

The model with the lowest RMSE employed PLSR, used the y-transform, using R as the independent variable and MSC as the pre-processing technique, see Table I. This model obtained an RMSE of 1.6142 %DM and an $RMSE_{pp}$ of 0.6102 in the transformed dimensional scale.

TABLE I
RMSE Of The 36 Models Created For %DM

		y		$log(y)$		$\sqrt{y}$		y^2	
Feature	PP[a]	PCR	PLSR	PCR	PLSR	PCR	PLSR	PCR	PLSR
R	SNV	2.19	1.62	2.21	1.62	2.20	1.62	2.18	1.62
	MSC	2.11	1.61	2.17	1.62	2.13	1.62	2.08	1.62
	None	2.12	1.65	2.16	1.67	2.14	1.78	2.09	1.66
$Log\left(\frac{1}{R}\right)$	SNV	2.26	1.65	2.28	1.70	2.26	1.67	2.25	1.63
	MSC	2.28	1.65	2.30	1.70	2.29	1.67	2.27	1.63
	None	2.23	1.71	2.29	1.76	2.25	1.73	1.98	1.68
1D	SNV	2.16	1.75	2.19	1.78	2.17	1.76	2.16	1.74
	MSC	2.14	1.76	2.17	1.79	2.15	1.63	2.12	1.75
	None	2.10	1.67	2.18	1.71	2.14	1.69	2.07	1.66

Note: [a]Pre-processing

Next, the best model for %MD is analyzed. Fig. 9 shows the histogram of the optimal number of components found in the double CV for the PLSR-y-R-SNV model. Therefore, finally the model used only 3 components.

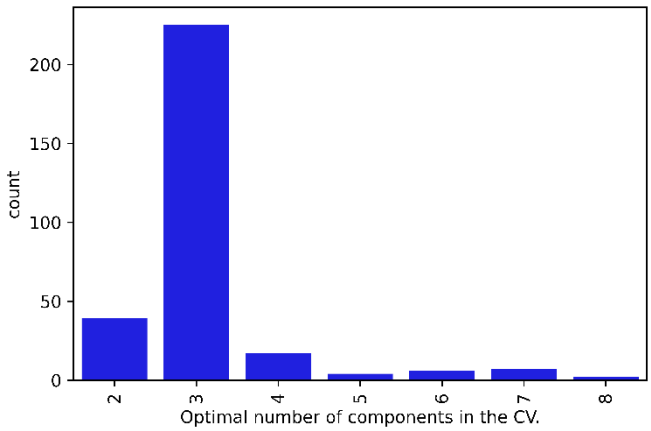

Fig. 9 Histogram of the optimal number of components in the double CV for the PLSR-y-R-MSC model.

Fig. 10 shows the MSE on the transformed scale of the variable for different model complexities in the Double CV. The gray line shows the MSE in each of the CVs, while the blue line represents the average of all the gray lines. The red dashed line shows the optimal number of components determined in Fig. 9. Finally, the cyan dashed line shows the MSE level in the test set.

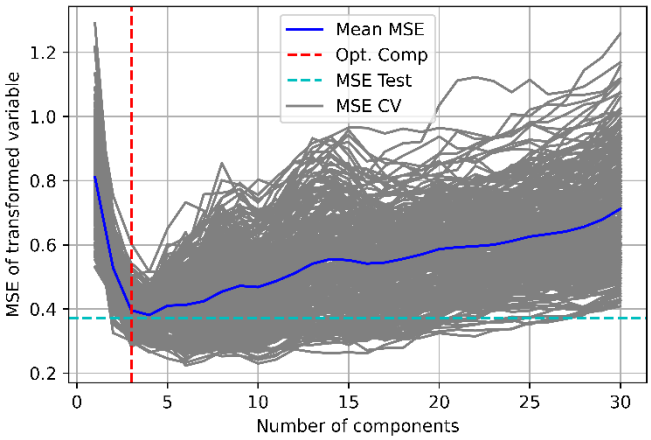

Fig. 10 MSE of transformed variable to different model complexity in Double CV.

Fig. 11 shows the predicted versus actual DM values. In the plot a trend can be observed in the blue line representing a perfect model. In gray color the predictions made in each of the CVs of the Double CV are shown. In addition, the predictions of the test set are represented with different colors corresponding to each mango.

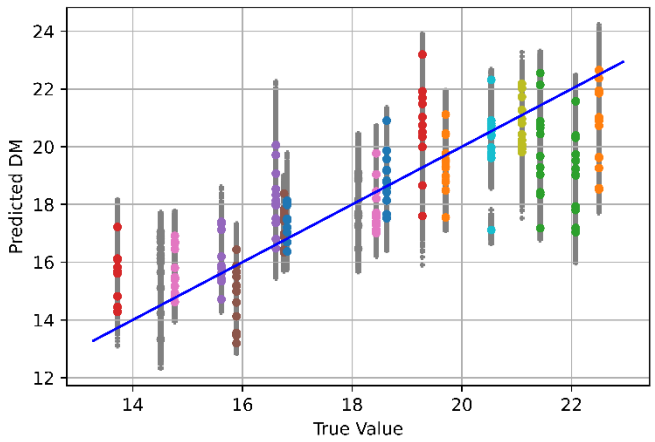

Fig. 11 DM Prediction Vs True value.

Fig. 12 shows the prediction errors versus the actual DM values. In the plot an average error close to zero can be observed. In gray color the prediction errors of each of the CVs of the Double CV are shown. In addition, the prediction errors of the test set are displayed with different colors corresponding to each mango.

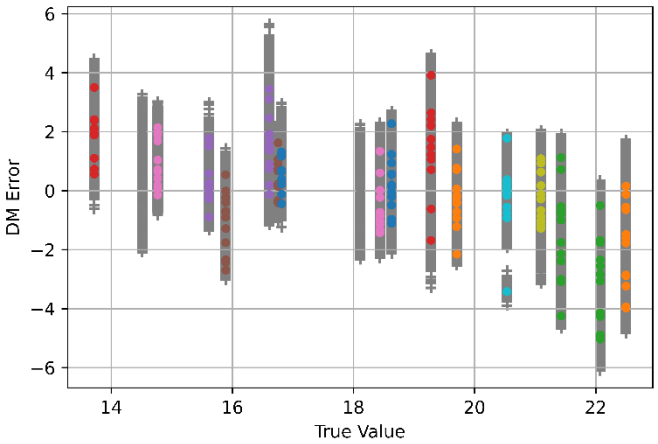

Fig. 12 DM Error Vs True value

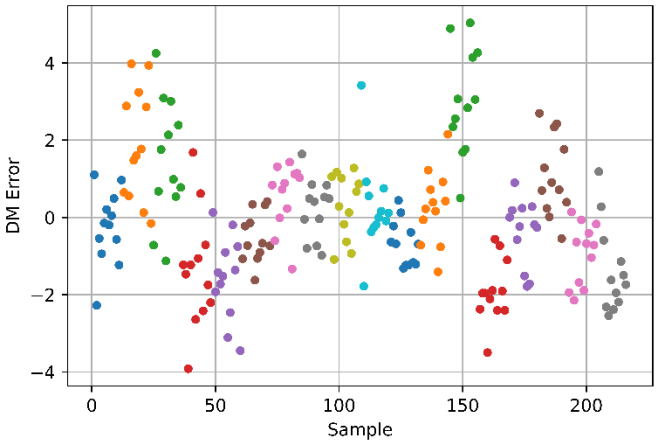

Fig. 13 DM Error Vs Sample

Fig. 13 shows the prediction errors versus sample number. A mean error close to zero and a relatively constant variance distribution can be observed in the plot. The prediction errors of the test set are plotted with different colors corresponding to each mango.

The results are analyzed from the mean RMSE and the range considering the standard deviation of the expected value according to (2)

$$Std = \hat{\sigma}/\sqrt{c} \tag{2}$$

Where Std is the standard deviation of the expected value, $\hat{\sigma}$ is standard deviation of the samples and c is the number of samples.

Table II shows the RMSE of the expected PCR and PLSR, as well as the ranges for the DM variable applying different transformations. The results showed evidence that PLSR has better metrics than PCR for all the transformations studied. On the other hand, y and y^2 transformations have shown evidence that on average they present better results than $log(1/R)$ transformation when using PCR. Additionally, it is shown that the y^2 transformation has presented on average better results than $log(1/R)$ when using PLSR.

TABLE II
AVERAGE AND RANGE OF RMSE APPLIED TO DIFFERENT TRANSFORMATION

Transformation	RMSE PCR	RMSE PCR ± 1*Std	RMSE PLSR	RMSE PLSR ± 1*Std
y	2.18	[2.16 2.20]	1.68	[1.66 1.70]
$log(y)$	2.22	[2.20 2.24]	1.71	[1.69 1.73]
$\sqrt{y}$	2.20	[2.18 2.22]	1.69	[1.67 1.71]
y^2	2.14	[2.11 2.17]	1.67	[1.66 1.69]

Note: c value is 9.

Table III shows the expected RMSEs of PCR and PLSR, as well as the ranges for the DM variable using different features. The results showed evidence that PLSR has better metrics than PCR for the different types of features. On the other hand, the use of $log(1/R)$ has shown that on average it has disadvantages with respect to other features when PCR is used. Additionally, the use of R has shown that on average it presents better results than $log(1/R)$ and $1D$ when PLSR is used.

TABLE III
AVERAGE AND RANGE RMSE APPLYING DIFFERENT TYPES OF FEATURE EXTRACTION.

Feature	RMSE PCR	RMSE PCR ± 1*Std	RMSE PLSR	RMSE PLSR ± 1*Std
R	2.15	[2.14 2.17]	1.65	[1.63 1.66]
$log(1/R)$	2.25	[2.23 2.27]	1.69	[1.68 1.70]
$1D$	2.15	[2.14 2.16]	1.73	[1.71 1.74]

Note: c value is 12.

Table IV shows the expected RMSE of PCR and PLSR, as well as the ranges for the DM variable applying different preprocessing techniques. The results of PLSR are better than

those of PCR using either preprocessing. On the other hand, there is sufficient evidence that SNV is detrimental when PCR is used. However, there is no evidence of the same when PLSR is used.

TABLE IV
AVERAGE AND RANGE OF RMSE APPLIED TO DIFFERENT PRE-PROCESSING TECHNIQUES

Pre-processing	RMSE PCR	RMSE PCR ± 1*Std	RMSE PLSR	RMSE PLSR ± 1*Std
SNV	2.21	[2.20 2.23]	1.68	[1.67 1.70]
MSC	2.19	[2.17 2.21]	1.68	[1.66 1.69]
None	2.15	[2.13 2.17]	1.70	[1.69 1.71]

Note: c value is 12

IV. CONCLUSIONS

We tested a total of 18 PCR and 18 PLSR models. A methodology based on a double CV was implemented. The internal CV was used to find the optimal number of components, a_{opt}, which was found with the one standard deviation rule.

The model with the lowest RMSE employed PLSR with 3 components, used y-transform, R-reflectance as independent variable and MSC as pre-processing technique. This model obtained an RMSE of 1.6142 %MS and an $RMSE_{pp}$ of 0.6102 in the transformed dimensional scale.

The y and y^2 transformations have shown evidence that on average they present better results than $log(1/R)$ transformation when using PCR. Additionally, it is shown that the y^2 transformation has presented on average better results than $log(1/R)$ when using PLSR. In addition, working directly with reflectance R has given good results. Not enough evidence has been found to claim that any preprocessing technique is better than another. Additionally, it can be stated that PLSR always showed equal or better results than PCR.

Finally, it was evidenced that it is possible to create models with good performance for Edwards mango by applying NIR spectroscopy to estimate dry matter.

ACKNOWLEDGMENT

We acknowledge the Universidad Tecnológica del Perú for its support throughout the project.

REFERENCES

[1] N. T. Anderson, K. B. Walsh, P. P. Subedi, and C. H. Hayes, "Achieving robustness across season, location and cultivar for a NIRS model for intact mango fruit dry matter content.," Postharvest Biol Technol, 2020.

[2] F. Fatima, M. Kaleem Baloch, O. Ullah, M. Asghar, and S. Iqbal, "Postharvest Quality and Shelf Life of Mango (Mangifera Indica L.) Fruit: As Affected by The Degree of Exposure to Sunlight," The Sceincetech, vol. 3, no. 4, 2022.

[3] H. M. Rizwan Iqbal and A. Hakim, "Classification and Grading of Harvested Mangoes Using Convolutional Neural Network," International Journal of Fruit Science, vol. 22, no. 1, pp. 95–109, 2022, doi: 10.1080/15538362.2021.2023069.

[4] N. D. Thong, N. T. Thinh, and H. T. Cong, "Mango classification system uses image processing technology and artificial intelligence.," 2019 International Conference on System Science and Engineering (ICSSE), pp. 45–52, 2019.

[5] D. Worasawate, P. Sakunasinha, and S. Chiangga, "Automatic Classification of the Ripeness Stage of Mango Fruit Using a Machine Learning Approach," AgriEngineering, vol. 4, no. 1, pp. 32–47, Mar. 2022, doi: 10.3390/agriengineering4010003.

[6] V. Cortés, C. Ortiz, N. Aleixos, J. Blasco, S. Cubero, and P. Talens, "A new internal quality index for mango and its prediction by external visible and near-infrared reflection spectroscopy," Postharvest Biol Technol, vol. 118, pp. 148–158, Aug. 2016, doi: 10.1016/j.postharvbio.2016.04.011.

[7] P. Mishra and D. Passos, "A synergistic use of chemometrics and deep learning improved the predictive performance of near-infrared spectroscopy models for dry matter prediction in mango fruit," Chemometrics and Intelligent Laboratory Systems, vol. 212, May 2021, doi: 10.1016/j.chemolab.2021.104287.

[8] P. Chaisrichonlathan and C. Chavapradit, "Durian maturity meter by dry weight," Acta Hortic, no. 1186, pp. 165–170, Nov. 2017, doi: 10.17660/ActaHortic.2017.1186.25.

[9] R. Singh Sidhu, S. A. Bound, and N. D. Swarts, "Influence of harvest maturity on fruit quality and storage potential of 'Scilate' apples," Acta Hortic, no. 1353, pp. 263–272, Dec. 2022, doi: 10.17660/ActaHortic.2022.1353.33.

[10] T. Nordey, J. Joas, F. Davrieux, M. Chillet, and M. Léchaudel, "Robust NIRS models for non-destructive prediction of mango internal quality," Sci Hortic, vol. 216, pp. 51–57, Feb. 2017, doi: 10.1016/j.scienta.2016.12.023.

[11] J. P. dos Santos Neto, M. W. D. de Assis, I. P. Casagrande, L. C. Cunha Júnior, and G. H. de Almeida Teixeira, "Determination of 'Palmer' mango maturity indices using portable near infrared (VIS-NIR) spectrometer," Postharvest Biol Technol, vol. 130, pp. 75–80, Aug. 2017, doi: 10.1016/j.postharvbio.2017.03.009.

[12] M. L. Ntsoane, M. Zude-Sasse, P. Mahajan, and D. Sivakumar, "Quality assesment and postharvest technology of mango: A review of its current status and future perspectives," Sci Hortic, vol. 249, pp. 77–85, Apr. 2019, doi: 10.1016/j.scienta.2019.01.033.

[13] M. Bizzani, D. William Menezes Flores, T. Bueno Moraes, L. Alberto Colnago, M. David Ferreira, and M. Helena Fillet Spoto, "Non-invasive detection of internal flesh breakdown in intact Palmer mangoes using time-domain nuclear magnetic resonance relaxometry," Microchemical Journal, vol. 158, p. 105208, Nov. 2020, doi: 10.1016/j.microc.2020.105208.

[14] P. Wanitchang, A. Terdwongworakul, J. Wanitchang, and N. Nakawajana, "Non-destructive maturity classification of mango based on physical, mechanical and optical properties," J Food Eng, vol. 105, no. 3, pp. 477–484, Aug. 2011, doi: 10.1016/j.jfoodeng.2011.03.006.

[15] S. Lihuan, W. Liu, Z. Xiaohong, H. Guohua, and Z. Zhidong, "Fabrication of electronic nose system and exploration on its applications in mango fruit (M. indica cv. Datainong) quality rapid determination," Journal of Food Measurement and Characterization, vol. 11, no. 4, pp. 1969–1977, Dec. 2017, doi: 10.1007/s11694-017-9579-1.

[16] Y.-Y. Pu and D.-W. Sun, "Combined hot-air and microwave-vacuum drying for improving drying uniformity of mango slices based on hyperspectral imaging visualisation of moisture content distribution," Biosyst Eng, vol. 156, pp. 108–119, Apr. 2017, doi: 10.1016/j.biosystemseng.2017.01.006.

[17] P. Rungpichayapichet, M. Nagle, P. Yuwanbun, P. Khuwijitjaru, B. Mahayothee, and J. Müller, "Prediction mapping of physicochemical properties in mango by hyperspectral imaging," Biosyst Eng, vol. 159, pp. 109–120, Jul. 2017, doi: 10.1016/j.biosystemseng.2017.04.006.

[18] D. Xu et al., "Hyperspectral Imaging for Evaluating Impact Damage to Mango According to Changes in Quality Attributes," Sensors, vol. 18, no. 11, p. 3920, Nov. 2018, doi: 10.3390/s18113920.

[19] X. Sun, P. Subedi, and K. B. Walsh, "Achieving robustness to temperature change of a NIRS-PLSR model for intact mango fruit dry matter content," Postharvest Biol Technol, vol. 162, p. 111117, Apr. 2020, doi: 10.1016/j.postharvbio.2019.111117.

[20] P. Mishra, E. Woltering, and N. el Harchioui, "Improved prediction of 'Kent' mango firmness during ripening by near-infrared spectroscopy supported by interval partial least square regression," Infrared Phys Technol, vol. 110, Nov. 2020, doi: 10.1016/j.infrared.2020.103459.

[21]S. Sohaib Ali Shah et al., “Towards fruit maturity estimation using NIR spectroscopy,” Infrared Phys Technol, vol. 111, Dec. 2020, doi: 10.1016/j.infrared.2020.103479.
[22]J. R. Castro-Suarez, S. P. Hernández-Rivera, and L. Pacheco-Londoño, “Detection of primary and secondary explosives using infrared spectroscopy and chemometrics,” in Proceedings of the LACCEI international Multi-conference for Engineering, Education and Technology, 2017, vol. 2017-July. doi: 10.18687/LACCEI2017.1.1.81.
[23]J. Oblitas-Cruz, Y. Cieza-Rimarachin, and W. Castro-Silupu, “Determination of semolina adulteration by NIR spectroscopy,” in Proceedings of the LACCEI international Multi-conference for Engineering, Education and Technology, 2022, vol. 2022-July. doi: 10.18687/LACCEI2022.1.1.69.
[24]J. R. Castro-Suarez, A. A. Pájaro-Payares, E. Espinosa-Fuentes, and E. Meza-Fuentes, “Vibrational detection of acetaminophen in commercials tablets by ATR-FTIR spectroscopy and Chemometrics,” in Proceedings of the LACCEI international Multi-conference for Engineering, Education and Technology, 2017, vol. 2017-July. doi: 10.18687/LACCEI2017.1.1.319.
[25]P. Mishra, D. N. Rutledge, J. M. Roger, K. Wali, and H. A. Khan, “Chemometric pre-processing can negatively affect the performance of near-infrared spectroscopy models for fruit quality prediction,” Talanta, vol. 229, Jul. 2021, doi: 10.1016/j.talanta.2021.122303.
[26]E. J. N. Marques, S. T. de Freitas, M. F. Pimentel, and C. Pasquini, “Rapid and non-destructive determination of quality parameters in the ‘Tommy Atkins’ mango using a novel handheld near infrared spectrometer,” Food Chem, vol. 197, pp. 1207–1214, Apr. 2016, doi: 10.1016/j.foodchem.2015.11.080.
[27]T. Nordey, F. Davrieux, and M. Léchaudel, “Predictions of fruit shelf life and quality after ripening: Are quality traits measured at harvest reliable indicators?,” Postharvest Biol Technol, vol. 153, pp. 52–60, Jul. 2019, doi: 10.1016/j.postharvbio.2019.03.011.
[28]A. Rizzolo, M. Vanoli, L. Spinelli, and A. Torricelli, “Non-destructive assessment of pulp colour in mangoes by time-resolved reflectance spectroscopy: Problems and solutions,” Acta Hortic, vol. 1119, pp. 147–154, Jun. 2016, doi: 10.17660/ActaHortic.2016.1119.20.
[29]Y. Q. Polinar, K. F. Yaptenco, E. K. Peralta, and J. U. Agravante, “Near-infrared spectroscopy for non-destructive prediction of maturity and eating quality of ‘Carabao’ mango (Mangifera indica L.) fruit,” Agricultural Engineering International: CIGR Journal, vol. 21, no. 1, p. 209, 2019, [Online]. Available: http://www.cigrjournal.org
[30]S. Saranwong, J. Sornsrivichai, and S. Kawano, “Prediction of ripe-stage eating quality of mango fruit from its harvest quality measured nondestructively by near infrared spectroscopy,” Postharvest Biol Technol, vol. 31, no. 2, pp. 137–145, 2004, doi: 10.1016/j.postharvbio.2003.08.007.
[31]S. N. Jha et al., “Nondestructive prediction of maturity of mango using near infrared spectroscopy,” J Food Eng, vol. 124, pp. 152–157, 2014, doi: 10.1016/j.jfoodeng.2013.10.012.
[32]P. P. Subedi, K. B. Walsh, and G. Owens, “Prediction of mango eating quality at harvest using short-wave near infrared spectrometry,” Postharvest Biol Technol, vol. 43, no. 3, pp. 326–334, Mar. 2007, doi: 10.1016/j.postharvbio.2006.09.012.
[33]A. Savitzky and M. J. E. Golay, “Smoothing and Differentiation of Data by Simplified Least Squares Pro,cedures,” Anal. Chem., vol. 36, no. 8, pp. 1627–1639, 1964
[34]R. G. Brereton, “Chemometrics: Data Analysis for the Laboratory and Chemical Plant.,” Journal of Analytical Chemistry, vol. 60, no. 10, pp. 994–996, Oct. 2005, doi: 10.1007/s10809-005-0223-6.
[35]J. Steinier, Y. Termonia, and J. Deltour, “Comments on Smoothing and Differentiation of Data by Simplified Least Square Procedure,” Anal. Chem., pp. 1906–1909, 1972.